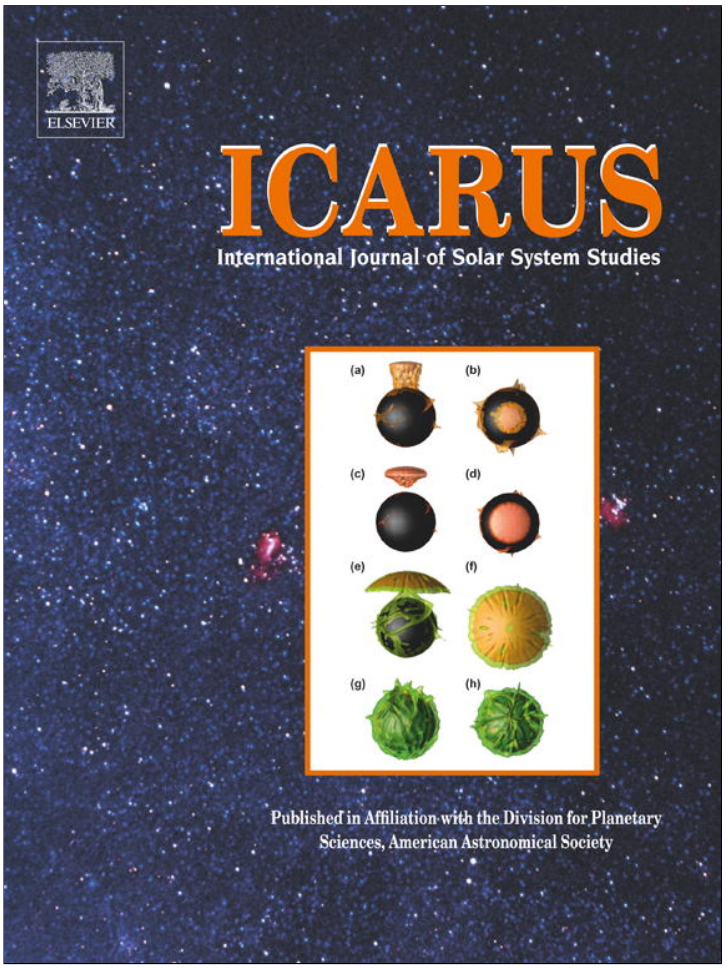

(This is a sample cover image for this issue. The actual cover is not yet available at this time.)

Icarus 221 (2012) 1079–1083

Contents lists available at SciVerse ScienceDirect

Icarus

journal homepage: www.elsevier.com/locate/icarus

Bidirectional reflectance spectroscopy 7
The single particle phase function hockey stick relation

Bruce Hapke *

Department of Geology and Planetary Science, University of Pittsburgh, Pittsburgh, PA 15260, United States

ARTICLE INFO

Article history:
Received 10 June 2012
Revised 21 September 2012
Accepted 2 October 2012
Available online 29 October 2012

Keywords:
Photometry Radiative transfer
Regoliths
Spectrophotometry

ABSTRACT

The measured volume-average single particle angular scattering functions of a large number of types of particle of interest for planetary regoliths in the visible-near-IR wavelength region can be represented to a reasonable approximation by two-parameter, double Henyey–Greenstein functions. When the two parameters of this function are plotted against one another they are found to be inversely correlated and lie within a restricted zone shaped like a hockey stick within the parameter space. The centroid of the zone is a curve that can be represented by a simple empirical equation. The wide variety of types of particles used to construct the plot implies that this equation may represent most of the particles found in regoliths. This means that when modeling the bidirectional reflectance of a regolith it may be possible to reduce the number of parameters necessary to specify the reflectance, and also to characterize the entire single particle phase function from observations at phase angles less than 90°. Even if the hockey stick relation has a finite width, rather than being a line, it restricts the parameter space that must be searched when fitting data. The curve should also be useful for forward modeling particle phase functions.

1. Introduction

When calculating the bidirectional reflectance of a planetary regolith it is necessary to know the volume average single particle angular scattering function, or single particle phase function (SPPF). This function is the average of the angular scattering functions of all the different types of the particles in the medium, including size, structure and composition. Although the scattering function of an individual particle can be quite complex, the averaging process generally smooths out large intensity excursions. In addition, the high, narrow, forward scattering Fraunhofer diffraction pattern of an isolated particle does not exist in a medium of closely-packed particles (Hapke, 1999, 2008, 2012). Thus the SPPF can often be represented by the two parameter, double Henyey–Greenstein (2PHG) function

$$p(g) = \frac{1+c}{2} p_{HGB}(g,b) + \frac{1-c}{2} p_{HGF}(g,b), \tag{1}$$

where

$$p_{HGB}(g,b) = \frac{1-b^2}{(1-2b\cos g + b^2)^{3/2}}, \tag{2}$$

$$p_{HGF}(g,b) = \frac{1-b^2}{(1+2b\cos g + b^2)^{3/2}}, \tag{3}$$

and g is the phase angle.

Typical 2PHG's are plotted in Fig. 1. The first term in Eq. (1) represents a back scattered lobe centered on $g = 0$, and the second term a forward scattered lobe centered on $g = 180°$. The shape parameter b describes the widths and heights of the lobes. The lobes are low and wide for small values of b, and high and narrow for large. The 2PHG function assumes that the shapes of both lobes are the same. The distribution of energy between the two lobes is specified by the asymmetry parameter c. Negative values of c mean that the particle is predominantly forward scattering, and positive values back scattering. (It should be noted that a certain amount of confusion exists in the literature concerning the definition of c. Some authors replace $(1 + c)/2$ by c and $(1 - c)/2$ by $(1 - c)$ in Eq. (1), while others do the opposite.)

Other properties of the 2PHG function are as follows. (i) It is normalized:

$$\frac{1}{4\pi}\int_0^\pi p(g) 2\pi \sin g\, dg = 1. \tag{4}$$

(Actually, each function $p_{HGB}(g)$ and $p_{HGF}(g)$ has the property that it is separately normalized, thus ensuring that Eq. (1) is automatically normalized for any value of c.) and (ii) The mean cosine of the scattering angle $\theta = \pi - g$, called the asymmetry factor, is

$$\langle \cos\theta \rangle = \frac{1}{4\pi}\int_0^\pi \cos\theta p(\theta) 2\pi \sin\theta d\theta = -bc. \tag{5}$$

(iii) The shape parameter b is restricted to the range $0 \leqslant b \leqslant 1$. (iv) The parameter c is restricted by the condition that $p(g)$ cannot be

* Address: University of Pittsburgh, 200 SRCC Bldg., 4107 O'Hara St., Pittsburgh, PA 15260, United States. Fax: +1 412 624 3914.
E-mail address: hapke@pitt.edu

0019-1035/$ - see front matter © 2012 Elsevier Inc. All rights reserved.
http://dx.doi.org/10.1016/j.icarus.2012.10.022

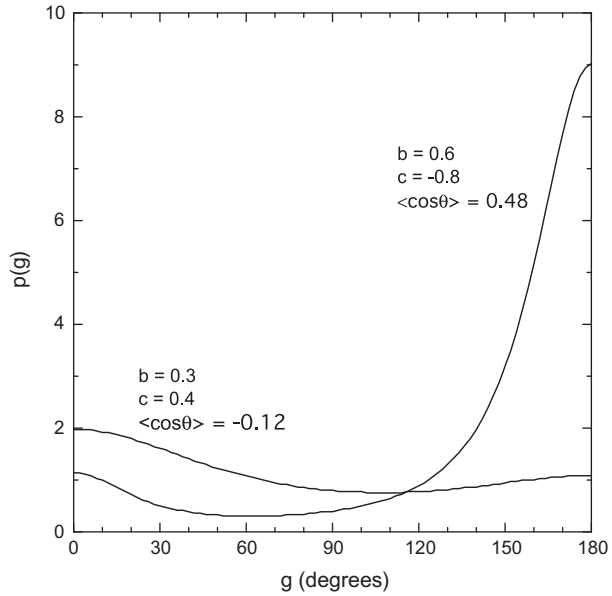

Fig. 1. Typical two parameter double Henyey–Greenstein functions, illustrating a forward and a back scattering particle. Values of the parameters are given next to each curve.

negative. Since $p(g)$ has extremes at $g = 0$ and 180°, it may readily be shown that this requires

$$|c| \leqslant \frac{1+3b^2}{b(3+b^2)}. \tag{6}$$

This condition is shown as the lines in Fig. 2. Only values of c between the lines are allowed.

The three parameter double Henyey–Greenstein function is identical to the 2PHG except that the shape parameters are allowed to be different for the two lobes. Hartman and Domingue (1998) investigated the two and three parameter functions. They concluded that, although the three parameter function usually gave a slightly better fit to measured SPPF's, the two parameter function fit was almost as good and sufficient for many purposes. In addition, it has the advantage of requiring fewer parameters.

McGuire and Hapke (1995) used the 2PHG function to characterize the SPPF's of 42 artificial planetary regolith analog particles constructed and measured by them. When they plotted c against b they found that the parameters were inversely correlated such that the points occupied a relatively small area shaped like the letter L, or like a hockey stick. Hapke (2012) fitted the centroid of this area by the empirical function

$$c = \left(\frac{0.05}{b-0.15}\right)^{3/4} - 1. \tag{7}$$

It is the purpose of this paper to investigate the c vs b correlation further. It will be shown that the correlation appears to be quite general for particles likely to be found in planetary regoliths, but that Eq. (7) must be replaced by a more general expression.

2. The hockey stick relation

Subsequently other authors measured the phase functions of particles and fitted 2PHG functions to them. The references to these studies are listed in Table 1 along with summary descriptions of the particles and other details of the measurements. Many of these authors also noted the inverse correlation between c and b in their data. Other persons besides those listed in Table 1 have

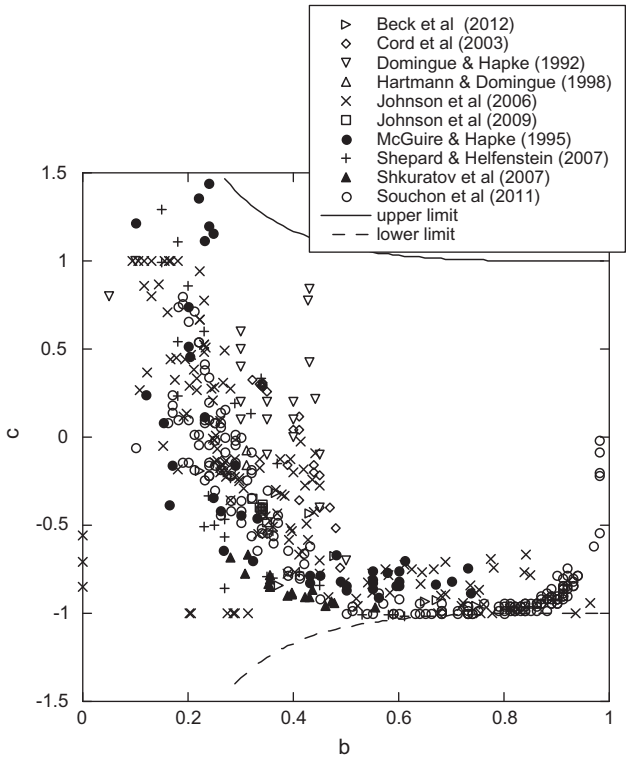

Fig. 2. Plot of c vs b for the 495 particles described in the text and Table 1. Particles whose phase functions have been measured directly are shown as filled circles and triangles. Particles whose functions have been found by fitting the IMSA model to reflectance measurements of powders are shown as open symbols, x's and crosses. Only values of c between the solid upper line and dashed lower line are allowed.

noted the inverse correlation (Mustard and Pieters, 1989; Sato et al., 2012; Kamei and Nakamura, 2002), but they either did not report parameters or did not fit 2PHG functions to their data and so their results are not included in the table.

The 2PHG functions were fitted to the measured SPPF values in two different ways in the papers listed in Table 1. In the first method Eq. (1) was fitted directly to measurements of the light scattered by individual particles, ignoring the diffraction peak. This direct method was used by McGuire and Hapke (1995) and Shkuratov et al. (2007). Shkuratov et al. (2007) fitted the equation to the small terrestrial particles that had been previously measured by the Amsterdam group (Munoz et al., 2000; Volten et al., 2001). The indirect or IMSA method was used in all the other papers listed in Table 1. In this method Eq. (1) was used as the SPPF in various versions of the isotropic multiple scattering approximation (IMSA) reflectance model of Hapke (1993, 2012). The bidirectional reflectances calculated from the models were then fitted to the measured reflectances of the materials in powder form by varying the parameters to minimize the rms difference between model and data.

(For completeness, it should be mentioned that Shkuratov et al. (2007) also retrieved 2PHG parameters from bidirectional reflectance measurements of powders of the Amsterdam group materials, but found that the values obtained using the IMSA and direct methods were different. The reasons for this are not clear. However, the conditions of the measurements of the powders allowed cooperative, coherent interactions between adjacent particles (Hapke, 2008), so that their effective SPPF's could be different from those when isolated. In the interest of relevance and brevity this will not be discussed further here. Only the parameter values from the direct method are considered in this paper.)

Table 1
Particles used to construct hockey stick.

Reference	Particle size	Wavelengths	Composition
Beck et al. (2012)	<1 mm	450–900 nm in 5 wavelengths	HED, carbonaceous and ordinary chondrites, lunar meteorites
Cord et al. (2003)	75–2000 μm in 4 sizes	603–1020 nm in 5 wavelengths	Basalt, altered palagonitic basalt, oxidized basaltic tephra
Domingue and Hapke (1992)	Europan regolith	470–580 nm in 4 wavelengths	Several types of terrains in Voyager images of Europa
Hartman and Domingue (1998)	Lunar regolith	B and V filters	Whole-disk observations of Moon (Rougier, 1933)
Johnson et al. (2006)	Martian regolith	432–1001 nm in 4 wavelengths	Several types of Martian terrains in Opportunity rover images
Johnson et al. (2009)	<1–1000 μm	450–950 nm in 4 wavelengths	Apollo 11 sample 10084
McGuire and Hapke (1995)	1 cm	448–690 nm in 3 wavelengths	Glass and resin artificial regolith particles, variety of shapes
Shepard and Helfenstein (2007)	<1–500 μm	450–700 nm in 3 wavelengths	Hawaiian sand, oolitic sand, quartz sand, clay, spodumene, several oxides
Shkuratov et al. (2007)	<1–100 μm	440 and 630 nm	Olivine, volcanic ash feldspar, loess, clay
Souchon et al. (2011)	45–2000 μm in 6 sizes	554–960 nm in 5 wavelengths	Basalt, basaltic sand, basaltic pyroclastics, andesitic pyroclastics, olivine, amorphous basaltic glass

Parameter errors are given in only some of the papers. When they are stated they have values between ±0.003 to ±0.2 in both b and c. However, in some cases these are formal fitting errors, which were obtained without taking account of possible errors in the measured data being fitted. These errors must be included because it is difficult (although not impossible) to measure absolute reflectance to much better than ±10% (e.g., Hapke, 1999), especially using spacecraft. Also, some of the fits used older versions of the model that did not include porosity effects (Hapke, 2008, 2012). Another potential source of error is that many of the observations were made at phase angles less than about 120°, so that the forward scattered lobe was poorly sampled. Thus, the smaller error values are probably overly optimistic, and it is suggested that the actual errors are more likely characterized by the high side of the stated values, probably closer to ±0.1 than to ±0.01.

The parameters reported in the papers listed in Table 1 are shown in Fig. 2, which plots c against b for 495 measurements of a wide variety of types of particles, including artificial regolith analogs, mineral separates, volcanic soils and derivatives, meteorites, and lunar, martian and European regoliths at several wavelengths. The parameters obtained using the direct method are plotted as filled circles and triangles. The parameters retrieved using the IMSA method are plotted as open symbols, x's and crosses.

With few exceptions, all the particles fall into a restricted hockey stick shaped region similar to that found by McGuire and Hapke (1995). There are three groups of outliers in Fig. 2. The first consists of three particles with $b = 0$ and $-0.8 < c < -0.6$. A particle with $b = 0$ scatters light isotropically, in which case c is indeterminate and meaningless. The second group contains six particles with b close to 1.00 and $-0.4 < c < 0$. However, particles with b nearly equal to 1.00 have forward and back scattering lobes that are so narrow and high as to be pathological. See Fig. 3, which plots the phase function corresponding to the point with $b = 0.98$, $c = -0.02$. It is not at all clear how such particles might be constructed. The third group consists of four particles with $b \sim 0.40$ and $0.2 < c < 0.8$ that lie above and outside the general hockey stick area. These are the values of the parameters found by Domingue and Hapke (1992) for the disk-integrated leading and trailing hemispheres of Europa, an icy satellite. However, the other parameters of this data set are for individual resolved areas on Europa, and all of these fall within the hockey stick region. The reason for the differences between the disk-integrated and disk-resolved parameters is unknown. Thus, there are reasons for believing that there may have been problems in the measurement or fitting processes for these outliers, as the authors have in some cases acknowledged.

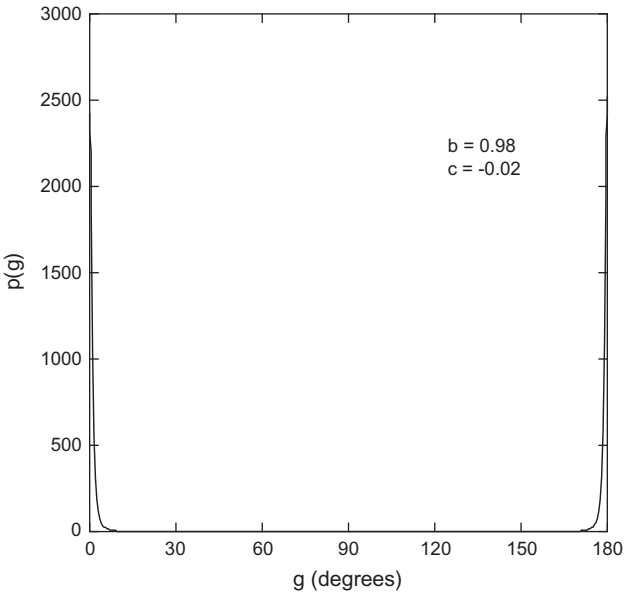

Fig. 3. Single particle phase function of a particle with $b = 0.98$ and $c = -0.02$.

Except for the outliers, the left ~5% of the diagram and the right half with $c \geqslant \sim -0.7$ seems to be forbidden. There is no mathematical reason for this, as the entire area between the two lines in Fig. 2 is allowed. Physically, it appears that nature abhors particles that scatter nearly isotropically (b small or zero) or ones with high, narrow lobes that scatter nearly symmetrically or in the backward direction (b large, $c \geqslant \sim 0$). This can be understood in terms of the particle structure, including shape, surface roughness and presence of internal scatterers. In order to be strongly forward scattering a particle must have a structure that readily transmits the incident light, which tends to pass through with only relatively small angular deviations, so that the peak tends to be narrow and high. However, in order to scatter light symmetrically or be a back scatterer a particle must have a high density of internal and/or external scattering structures; these scatter light through a wide range of angles, so that the peak tends to be wide and low.

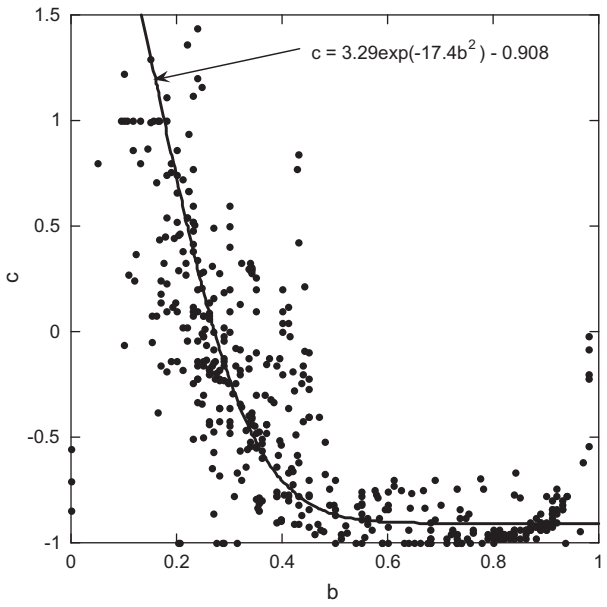

Fig. 4. Plot of c vs b. The points are the same 495 data values of Fig. 1. The solid line is Eq. (8).

The large number of data points and particle types allows an equation that is more general than Eq. (7) to be fitted to the centroid of the hockey stick. Over the parameter range ($0 < b < 1$, $-1 < c < 1.5$) the centroid can be represented by the empirical function

$$c = 3.29\exp(-17.4b^2) - 0.908. \quad (8)$$

This equation is shown as the solid line in Fig. 4, along with the same points as Fig. 2. Solving Eq. (8) for b gives

$$b = \left[\frac{1}{17.4}\ln\frac{3.29}{0.908 + c}\right]^{1/2}. \quad (9)$$

The root mean square average of the differences between the data points and Eq. (8) are $\Delta c = \pm 0.084$ for the nearly horizontal "blade" of the hockey stick region and $\Delta b = \pm 0.064$ for the nearly vertical "handle". These values are similar to the ±0.1 errors of the data points estimated above. This suggests that if the parameters could be measured with perfect accuracy they would fall into a narrow strip, or even a line, close to Eq. (8), rather than occupying the wide region of Fig. 4. Eq. (8) may represent an actual physical relation that describes the distribution of energy between the forward and back scattering lobes of the SPPF of planetary regolith particles.

3. Discussion and conclusions

(1) The wide variety of types of particles that contribute to Fig. 2 implies that the 2PHG, Eq. (1), is representative of regolith particles. Although the two-parameter double Henyey–Greenstein function does not describe the single particle phase function of any single particle exactly, it appears to be adequate to characterize most of the particles found in planetary regoliths.

(2) The parameters measured using the direct and IMSA methods appear to be members of the same population. This implies that regolith SPPF's can be reliably retrieved using the IMSA model. (However, particles near a wavelength in size may exhibit cooperative mutual interactions (Hapke, 2008) that may make their SPPF's in a regolith differ from those when isolated.)

(3) The inverse correlation between b and c noted by McGuire and Hapke (1995) appears to be quite general.

(4) There are no major differences between the distributions of the 2PHG parameters within the hockey stick region for the different types of particles, so that the hockey stick relation may be general.

(5) A major question is whether the scatter of the points in Fig. 4 about the line represented by Eq. (8) is real or noise. Is the hockey stick a line or does it have a considerable width about the line? If the latter, what is the width? If the thickness is small, then inserting Eq. (8) into Eq. (1) would allow the SPPF to be defined by a single parameter b, thus reducing the number of parameters necessary to fit photometric observations of surfaces of objects in the Solar System. Most orbiting spacecraft cameras are nadir-looking, which means that the reflectance of a planetary surface is difficult to measure at phase angles much larger than 90°, so that the forward scattering lobe of the SPPF cannot be observed directly. If it could be found using Eq. (8) this would be quite valuable.

To give an example, an analysis of Lunar Reconnaissance Orbiter Camera data at phase angles less than 90° using a single-lobed Henyey–Greenstein function found that $b = 0.28$ at 415 nm and $b = 0.29$ at 556 nm for a representative area in the lunar highlands (Hapke et al., 2012). Inserting these values into Eq. (8) gives $c = 0.05$ and 0.13, respectively. For comparison, Hartman and Domingue (1998) analyzed Rougier's (1933) whole disk data for the Moon and found $(b, c) = (0.31, 0.07)$ in the B filter and $(0.31, 0.16)$ in the V filter. At each wavelength the values are the same within the measurement errors.

However, Eq. (8) must be used with care because the handle of the hockey stick is nearly vertical. Thus, a medium with b on the left hand side of the diagram requires the determination of b with high accuracy in order to find c with small error.

(6) Even if the hockey stick is not a line it is still useful because it greatly restricts the parameter space that must be searched when fitting data. Eq. (8) should provide good starting values for data fitting algorithms.

(7) The equivalent slab model (Hapke, 2012) can be used to calculate the single scattering albedo and c of an irregular particle from the size, refractive index and density of internal scatterers, but it does not give b. If the width of the hockey stick is small b can be found from Eq. (9), and inserted into Eq. (1) to give the SPPF of the particle.

(8) Eq. (8) is a conjecture, put forth with the intention that it will stimulate more careful measurements, observations and theoretical calculations, which may determine whether the hockey stick is truly a line or has a finite width, and the range of its generality.

Acknowledgments

This study was supported by the National Aeronautics and Space Administration Lunar Reconnaissance Orbiter Project. I thank Mauro Ciarniello, Paul Helfenstein and an anonymous reviewer for constructive comments and suggestions.

References

Beck, P., Pommeral, A., Thomas, N., Schmidt, B., Moynier, F., Barat, J.-A., 2012. Photometry of meteorites. Icarus 218, 364–377.

Cord, A., Pinet, P., Daydou, Y., Chevrel, S., 2003. Planetary regolith surface analogs: Optimized determination of Hapke parameters using multi-angular spectro-imaging laboratory data. Icarus 165, 414–427.

Domingue, D., Hapke, B., 1992. Disk-resolved photometric analysis of European terrains. Icarus 99, 70–81.
Hapke, B., 1993. Theory of Reflectance and Emittance Spectroscopy, first ed. Cambridge University Press, Cambridge, UK.
Hapke, B., 1999. Scattering and diffraction of light by particles in planetary regoliths. J. Quant. Spectrosc. Radiat. Transf. 61, 565–581.
Hapke, B., 2008. Bidirectional reflectance spectroscopy 6. Effects of porosity. Icarus 195, 918–926.
Hapke, B., 2012. Theory of Reflectance and Emittance Spectroscopy, second ed. Cambridge University Press, Cambridge, UK.
Hapke, B., Denevi, B., Sato, H., Braden, S., Robinson, M., 2012. The wavelength dependence of the lunar phase curve as seen by the Lunar Reconnaissance Orbiter wide-angle camera. J. Geophys. Res. – Planets 117, E001115, doi: http://dx.doi.org/10.1029/2011JE003916.
Hartman, B., Domingue, D., 1998. Scattering of light by individual particles and the implications for models of planetary surfaces. Icarus 131, 421–448.
Johnson, J. et al., 2006. Spectrphotometric properties of materials observed by Pancam on the Mars Exploration Rovers: 2. Opportunity. J. Geophys. Res. Planets 111, E12S16, doi: http://dx.doi.org/10.1029/2006JE002762.
Johnson, J., Shepard, M., Paige, D., Foote, E., Grundy, W., 2009. Spectrogoniometric measurements and modeling of Apollo 11 soil 10084. Lunar Planet. Sci. 40. Abstract 1427.
Kamei, A., Nakamura, A., 2002. Laboratory study of the bidirectional reflectance of powdered surfaces: On the asymmetry parameter of asteroid photometric data. Icarus 156, 551–561.
McGuire, A., Hapke, B., 1995. An experimental study of light scattering by large irregular particles. Icarus 113, 134–155.
Munoz, O., Volten, H., de Haan, J., Vassen, W., Hovenier, J., 2000. Experimental determination of scattering matrices of olivine and Allende meteorite particles. Astron. Astrophys. 360, 777–788.
Mustard, J., Pieters, C., 1989. Photometric phase functions of common geologic minerals and applications to quantitative analysis of mineral mixture reflectance spectra. J. Geophys. Res. 94 (B10), 13,619–13,644.
Rougier, M., 1933. Total photoelectric photometry of the Moon. Ann. Obs. Strassbourg 2, 205–339.
Sato, H., Denevi, B., Robinson, M., Hapke, B., McEwen, A., 2012. Photometric parameter maps of the Moon from LROC WAC observations. Lunar Planet. Sci. 43. Abstract 1771.
Shepard, M., Helfenstein, P., 2007. A test of the Hapke photometric model. J. Geophys. Res. 112, E03001. http://dx.doi.org/10.1029/2005JE002625.
Shkuratov, Y., Bondarenko, S., Kaydash, V., Videen, G., Munoz, O., Volten, H., 2007. Photometry and polarimetry of particulate surfaces and aerosol particles over a wide range of phase angles. J. Quant. Spectrosc. Radiat. Transf. 106, 487–508.
Souchon, A. et al., 2011. An experimental study of Hapke's modeling of natural granular surface samples. Icarus 215, 313–331.
Volten, H., Munoz, O., Rol, E., de Haan, J., Vassen, W., Hovenier, J., 2001. Scattering matrices of mineral aerosol particles at 441.6 nm and 632.8 nm. J. Geophys. Res. 106, 17375–17401.